NASA TECHNICAL MEMORANDUM

NASA TM X-71475

NASA TM X-71475

(NASA-TM-X-71475) OPTIMIZATION OF SELF-ACTING HERRINGBONE JOURNAL BEARING FOR MAXIMUM STABILITY (NASA) 14 p HC $3.00 CSCL 13I

N74-11302

Unclas

G3/15 21990

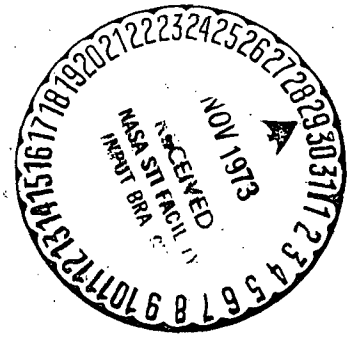

OPTIMIZATION OF SELF-ACTING HERRINGBONE JOURNAL BEARINGS FOR MAXIMUM STABILITY

by David P. Fleming and Bernard J. Hamrock
Lewis Research Center
Cleveland, Ohio 44135

TECHNICAL PAPER proposed for presentation at Sixth International Gas Bearing Symposium
Southampton, England, March 26-29, 1974

OPTIMIZATION OF SELF-ACTING HERRINGBONE JOURNAL BEARINGS FOR MAXIMUM STABILITY

by

David P. Fleming

and

Bernard J. Hamrock

NASA-Lewis Research Center
Cleveland, Ohio, U.S.A.

E-7793

SUMMARY

Groove parameters were determined to maximize the stability of herringbone grooved journal bearings. Parameters optimized were groove depth, width, length, and angle. Optimization was performed using a small eccentricity, infinite groove analysis in conjunction with: 1) a previously developed Newton-Raphson procedure for bearings with the smooth member rotating or with the grooved member rotating at low compressibility numbers; 2) a newly-developed vector technique for bearings with the grooved member rotating at high compressibility numbers.

The design curves in this report enable one to choose the optimum bearing for a wide range of operating conditions. These include: 1) compressibility numbers from 0 (incompressible) to 80; 2) length to diameter ratios from 1/4 to 2; and 3) smooth or grooved member rotating.

Compared to bearings optimized to maximize load capacity, bearings optimized for stability: 1) allow a thousandfold increase in bearing-supported mass in some cases before onset of instability (the most dramatic increases are for bearings with small L/D operating at high compressibility numbers); 2) lose no more than 77-percent of their load capacity in any case studied. Stability is much greater when the grooved member rotates.

NOMENCLATURE

A,B	numerical factors
b_g	width of groove
b_r	width of ridge
D	diameter of journal
$\overline{E}$	change in groove parameter vector
e	eccentricity of journal
f_r	radial load capacity of herringbone journal bearing
F_r	dimensionless radial load capacity
	$f_r/\epsilon p_a LD$ for compressible lubricant
	$2f_r h_r^2/3\mu\epsilon LD^3\omega$ for incompressible lubricant
h_g	film thickness in groove region when journal is concentric
h_r	film thickness in ridge region when journal is concentric
H	h_g/h_r = film thickness ration
L	length of journal
L_1	total axial length of groove
M	dimensionless stability parameter
	$mp_a(h_r/R)^5/2L\mu^2$ for compressible lubricant
	$3m\omega(h_r/R)^3/L\mu = M_{comp.}\Lambda$ for incompressible lubricant
m	mass supported by bearing
N	number of grooves
p_a	ambient pressure
R	radius of journal
α	$b_g/(b_g+b_r)$ = groove width ratio
β	groove angle
γ	L_1/L = groove length ratio
ϵ	e/h_r = eccentricity ratio
θ	angular coordinate
Λ	bearing compressibility number $6\mu\omega R^2/p_a h_r^2$
μ	dynamic viscosity of lubricant
ω	angular velocity
∇	gradient operator

INTRODUCTION

More than any other factors, self-excited whirl instability and low load capacity limit the usefulness of gas lubricated self-acting journal bearings. The whirl problem is the tendency of the journal center to orbit the bearing center at an angular speed less than or equal to half that of the journal about its own center. In many cases the whirl amplitude is large enough to cause destructive contact of the bearing surfaces.

The low load capacity of self-acting gas lubricated journal bearings is also a serious concern in many applications. Unlike liquid lubricants, a gaseous lubricant changes its density as it passes through the bearing. This so-called compressibility effect results in a "terminal" load condition. That is, the load capacity does not increase indefinitely with speed, but quickly approaches a fixed value.

In quest of a bearing which would overcome the two problems of self-excited whirl instability and low load capacity, Vohr and Chow (1) theoretically investigated a herringbone grooved journal bearing. They obtained a solution for bearing load capacity valid for small displacements of the journal center from the bearing center. An additional assumption was that the number of grooves was large enough that local pressure variations across a groove-ridge pair could be ignored. One of the conclusions obtained from the Vohr and Chow analysis is that in contrast to a plain bearing the load capacity of a herringbone grooved journal bearing increases without limit with increase in speed. Furthermore, the herringbone grooved journal bearing may not suffer from the self-excited whirl instability that is normally associated with unloaded plain bearings. Malanoski (2) and Cunningham et al. (3) and (4) experimentally verified the above conclusions of Vohr and Chow.

Therefore, it has been shown that the self-acting herringbone journal bearing has highly desirable characteristics, namely that of high load capacity and that of operating in a whirl free condition. A remaining problem is that of obtaining optimum herringbone journal bearing configurations for a wide range of bearing operating conditions. Hamrock and Fleming (5) determined groove parameters to maximize the radial load component of the herringbone bearing. The objective of the present work is to determine groove parameters which will maximize the bearing's stability, or resistance to self-excited whirl. This will be done utilizing the analysis of Vohr and Chow (1). Results are to be applicable for operating conditions ranging from incompressible to highly compressible lubrication ($\Lambda = 80$), and for bearing length-diameter ratios of 1/4 to 2.

BEARING DESCRIPTION

Figure 1 shows the bearing to be studied. Note that the bearing has angled, shallow grooves in the journal surface. The grooves can be partial as shown or extend the complete length of the bearing. Also, the grooves can be placed in the rotating or non-rotating surface. The purpose of these grooves is to pump fluid toward the center of the bearing thereby increasing the lubricant pressure in the bearing. This self pressurization can increase the load capacity over that of a smooth bearing; it is also responsible for the herringbone bearing's good stability. The bearing shown in Figure 1 is unidirectional, that is, it pumps inwardly for only one direction of rotation.

From Figure 1 the film thickness in the groove region is h_g and in the ridge region h_r. Also, the groove width is defined as b_g and the ridge width is defined as b_r. The analysis of (1) indicates that the groove parameters to be optimized are:

1. The film thickness ratio (H) which is equal to the film thickness in the groove region divided by the film thickness in the ridge region when the bearing is concentric ($H = h_g/h_r$).

2. The groove width ratio (α) which is equal to the width of the groove region divided by the width of the groove-ridge pair ($\alpha = b_g/(b_g+b_r)$).

3. The groove angle (β).

4. The groove length ratio (γ) which is equal to the length covered by grooves divided by the overall length of the bearing ($\gamma = L_1/L$).

In Figure 1 the number of grooves is six. However, the Vohr and Chow analysis (1) assumes essentially an infinite number of grooves. Reference (6) develops a criterion for minimum number of grooves such that the infinite groove analysis yields valid results. This criterion indicates that the minimum number of grooves placed around the journal can be represented conservatively by

$$N \geq \frac{\Lambda}{5} \tag{1}$$

where N = number of grooves

$\Lambda = \dfrac{6\mu\omega R^2}{p_a h_r^2}$ = bearing compressibility number

OPTIMIZING PROCEDURE

The problem is to maximize the bearing stability M by optimizing the groove parameters H, α, γ, and β. As previously mentioned, the small eccentricity analysis of Vohr and Chow (1) is used. Stability is then determined for a particular configuration by the spectral analysis method of Pan (7). The optimization procedure is outlined only briefly here. Further details are in reference (8).

Basically, two different procedures were used, depending on the characteristics of the particular bearing being optimized. For the bearing having the smooth member rotating, and for the bearing with the grooved member rotating with low compressibility numbers, the method of (5) was used. In this method, one determines groove parameters such that

$$\frac{\partial M}{\partial H} = \frac{\partial M}{\partial \alpha} = \frac{\partial M}{\partial \gamma} = \frac{\partial M}{\partial \beta} = 0 \tag{2}$$

where M is a dimensionless stability parameter, using the Newton-Raphson procedure of solving simultaneous equations. This procedure is described in (9); in addition to its use in (5) it was used in optimizing a Rayleigh step thrust bearing (10).

When the smooth member of the bearing rotates, or the grooved member rotates with low compressibility number Λ, the stability decreases monotonically with increasing Λ, as shown in Figure 2(a). With the grooved member rotating, stability is no longer monotonic at higher Λ, as shown in Figure 2(b). (These characteristics are also shown in (2).) Thus, if one imposes the requirement that a bearing must operate at all Λ values less than the value in question (as the bearing must certainly be started and stopped occasionally) it follows that a proper optimization must maximize the minimum value of stability from $\Lambda = 0$ to the Λ of interest. This being the case, the Newton-Raphson method as used previously will not suffice.

Two cases present themselves. In the first, for moderate compressibility numbers (e.g., $\Lambda = 10$ for $L/D = 2$) the optimum stability curve is of the form shown for $\Lambda = 5.6$-14 in Figure 2(b). If one needs to operate at a maximum Λ of 10, then the minimum stability at $\Lambda = 5.6$ is the governing factor. In this case, the Newton-Raphson optimization can be applied at the Λ value where the minimum stability occurs. Since a change in groove parameters may change the Λ value where minimum stability occurs, this Λ value is recomputed at each iteration using a Newton-Raphson root finder.

For operation at high compressibility numbers a completely different technique is required as will be illustrated. Refer to the $\Lambda = 80$ curve of Figure 2(b). For these groove parameters, stability decreases with increasing Λ at low values of Λ. A relative minimum is reached at $\Lambda = 6$; M then increases, becoming unbounded near $\Lambda = 26$. Another relative minimum occurs at $\Lambda = 38$ and M is again unbounded near $\Lambda = 54$. Stability then decreases rapidly with increasing Λ.

In attempting to optimize the bearing, one finds that, if the groove parameters are adjusted to increase the relative minimum at $\Lambda = 6$, then the stability at $\Lambda = 80$ decreases. Thus, one must look at the stability for both Λ values simultaneously.

The methods of vector analysis are used here. The greatest rate of change of a function occurs along the gradient of that function. Refer again to the $\Lambda = 80$ curve of Figure 2(b) and denote by Λ_m and M_m the compressibility number and stability at the relative minimum ($\Lambda = 6$ in Figure 2(b)). Denote by Λ_1 and M_1 the compressibility number and stability at the compressibility number of interest ($\Lambda = 80$ in this example). In light of the foregoing discussion, it is evident that maximum stability over the range $0 - \Lambda_1$ will be attained when $M_m = M_1$. The technique is then to calculate the gradient of M at $\Lambda = \Lambda_m$ and $\Lambda = \Lambda_1$. A change is then made in the vector of independent variables (H, α, γ, β) by taking a linear combination of the two gradients just calculated so that the new M_m and M_1 will be equal and increased over the original values. This procedure is applied repeatedly, until further application no longer increases M_m and M_1.

The specific expressions to carry out this technique will now be presented. Denote by M_p the new value of M at Λ_1 and Λ_m and by $\bar{E}$ the change in the vector of independent variables. Then

$$M_p = M_1 + \bar{E} \cdot \nabla M_1 = M_m + \bar{E} \cdot \nabla M_m \tag{3}$$

But $\bar{E}$ is to be a linear combination of the two gradients:

$$\bar{E} = A \nabla M_m + B \nabla M_m \tag{4}$$

where A and B are scalars. Equations (3) and (4) are combined and solved for B:

$$B = \frac{M_1 - M_m - A \nabla M_1 \cdot (\nabla M_1 - \nabla M_m)}{\nabla M_m \cdot (\nabla M_1 - \nabla M_m)} \tag{5}$$

In the computer program used to perform the calculations, A is first chosen equal to 1 and $\bar{E}$ calculated by Equations (5) and (4). The magnitudes of the components of $\bar{E}$ (ΔH, $\Delta\alpha$, $\Delta\gamma$, $\Delta\beta$) are then compared with a maximum change to be allowed. If any components exceed these maxima, A is adjusted and $\bar{E}$ recomputed. The maxima are reduced as the computer "homes in" on the optimum. A five percent change in groove parameters was generally the maximum allowed at the beginning of the optimization procedure. At each iteration, Λ_m is recalculated using a Newton-Raphson root finder.

RESULTS

Tables I and II present optimum herringbone groove parameters (H, α, γ, β) to maximize stability over the range from $\Lambda = 0$ to the Λ value listed in the tables. Table I is for bearings with the smooth member rotating and Table II for bearings with the grooved member rotating. The tables cover an operating range from incompressible lubrication ($\Lambda = 0$) to $\Lambda = 80$, and length to diameter ratios of 1/4, 1/2, 1, and 2. In addition to the resultant stability, the tables show the calculated radial load component F_r and the ratios of stability and load to the respective quantities of the maximum load bearings of (5). Figures 3 to 8 are plotted from the data in Tables I and II. The maximum groove depth ratio considered was $H = 4$ and the maximum groove width ratio was $\alpha = .6$. These were considered to be reasonable upper limits for practical bearing manufacture.

Tables I and II show that the improvement in stability over that of the maximum load bearing generally increases with compressibility number and decreases with increasing length to diameter ratio. Stability improvement is greater for the bearing with the grooved member rotating. For $\Lambda = 80$ and $L/D = 1/4$ and $1/2$, the stability increase is over 3 orders of magnitude.

For the case of L/D = 1 with the smooth member rotating, two local optima were observed at $\Lambda = 80$. The one shown in Table I is that which gave the greater stability. It is possible that more than one local optimum exists for other cases as well. It was considered impractical to survey the entire possible range of all of the four parameters (H, α, γ, β) to determine optimum values. Instead, the optimization procedure was started from the maximum load solution (5) for the incompressible case. For $\Lambda = 1$ and higher, the optimization was started from the stability solution for the next lower Λ. It is felt that the use of this method is justified by the results, since the groove parameters determined yield bearings substantially more stable than the maximum load bearings of (5).

Radial load capacity, relative to the maximum load bearings, decreases with increasing compressibility number. In contrast to the thousandfold increase in stability, however, the greatest loss in load capacity is 77 percent.

Figure 3 shows the stability attained by the optimized bearings. Stability with the grooved member rotating is always higher than with the smooth member rotating. The difference becomes greater at higher compressibility numbers. The greatest difference is at $\Lambda = 80$ for L/D = 1 where the stability of the bearing with the grooved member rotating is some 77 times that of the bearing with the smooth member rotating.

For bearings with the grooved member rotating, there appears to also be an optimum length to diameter ratio. Maximum stability occurs for L/D = 1. This is not the case when the smooth member rotates; stability increases continuously as L/D increases from 1/4 to 2.

There are horizontal portions in each of the stability curves for the grooved member rotating. This occurs because of the non-monotonic behavior of the stability with compressibility number, as illustrated in Fig. 2(b). For compressibility numbers just to the right of the relative minimum in the curve, the governing stability over the range from 0 to the Λ of interest is the stability at the minimum, as discussed in the section OPTIMIZING PROCEDURE.

As shown by the $\Lambda = 80$ curve of Fig. 2(b), stability changes very rapidly with compressibility number at high Λ. This means that, practically, there is a limiting compressibility number beyond which instability ensues for any value of M. However, to the authors' knowledge, instability in this region of the stability map has not been observed experimentally.

It should also be noted that stability is quite sensitive to changes in groove parameters. Because of this and the manufacturing tolerances that must be allowed, a conservative design (M less than the theoretical stability limit by a factor of 2 or more) is recommended for bearings with the grooved member rotating at high Λ.

Radial load capacities of the optimized bearings are shown in Fig. 4. In common with the maximum load bearings of (5), radial load capacity generally increases with increasing length to diameter ratio and is higher when the smooth member rotates.

Figures 5-8 plot the optimum groove parameters as a function of compressibility number. It may be noted that, except for groove length ratio γ, the parameters for the bearing with grooved member rotating generally vary over a much wider range than for the smooth member rotating. Again, this is believed to be the result of the non-monotonic behavior of the stability curves, as discussed above. Groove length ratio is an exception to this wider variability. The fully grooved bearing ($\gamma = 1$) was optimum for nearly all the cases studied when the grooved member rotated. Experimental data (3) appear to verify this result.

CONCLUDING REMARKS

Optimum groove configurations were determined to maximize the stability of herringbone grooved journal bearings. Design curves presented enable one to find the optimum herringbone bearing for a wide range of operating conditions. These range from

incompressible lubrication to gas lubrication at high compressibility numbers, for either smooth or grooved members rotating, and for length to diameter ratios of 1/4, 1/2, 1, and 2.

Bearings with the grooved member rotating are substantially more stable than with the smooth member rotating, especially at high compressibility numbers. The bearing configurations derived herein are also much more stable than the maximum load bearing configurations derived by the authors in an earlier report. Again, the stability increase is greater at higher compressibility numbers.

REFERENCES

1. Vohr, J. H., and Chow, C. Y.: "Characteristics of Herringbone-Grooved, Gas-Lubricated Journal Bearings". Journal of Basic Engineering, 87, 3 pp. 568-578. (September, 1965).

2. Malanoski, S. B.: "Experiments on an Ultrastable Gas Journal Bearing". Journal of Lubrication Technology, 89, 4 pp. 433-438. (October, 1967).

3. Cunningham, R. E., Fleming, D. P., and Anderson, W. J.: "Experimental Stability Studies of the Herringbone-Grooved Gas-Lubricated Journal Bearing". Journal of Lubrication Technology, 91, 1 pp. 52-59. (January, 1969).

4. Cunningham, R. E., Fleming, D. P., and Anderson, W. J.: "Experimental Load Capacity and Power Loss of Herringbone-Grooved Gas-Lubricated Journal Bearings". Journal of Lubrication Technology, 93, 3 pp. 415-422. (July, 1971).

5. Hamrock, B. J., and Fleming, D. P.: "Optimization of Self-Acting Herringbone Grooved Journal Bearings for Maximum Radial Load Capacity". Gas Bearing Symposium, University of Southampton. (March, 1971).

6. Rieger, N. F., Ed.: "Design of Gas Bearings, Vol. 1 - Design Notes". p. 6.1.35. Mechanical Technology, Inc. (1966).

7. Pan, C. H. T.: "Spectral Analysis of Gas Bearing Systems for Stability Studies". Dynamics and Fluid Mechanics, vol. 3, Part 2 of Developments in Mechanics. pp. 431-447. John Wiley & Sons. (1965).

8. Fleming, D. P., and Hamrock, B. J.: "Optimization of Self-Acting Herringbone Grooved Journal Bearings for Maximum Stability". Proposed NASA Technical Note.

9. Scarborough, J. B.: "Numerical Mathematical Analysis". Sixth ed. Johns Hopkins Press. (1966).

10. Hamrock, B. J.: "Optimization of Self-Acting Thrust Bearings for Load Capacity and Stiffness". NASA TN D-5954 (1970).

TABLE I. HERRINGBONE GROOVE PARAMETERS TO MAXIMIZE STABILITY - SMOOTH MEMBER ROTATING

	INCOM-PRESSIBLE SOLUTION	COMPRESSIBLE SOLUTION BEARING COMPRESSIBILITY NUMBER Λ						LENGTH TO DIAMETER RATIO L/D
		1	5	10	20	40	80	
Film Thickness Ratio H	2.68	2.67	2.62	2.57	2.52	2.47	2.5	1/4
Groove Width Ratio α	.469	.466	.454	.441	.421	.397	.38	
Groove Length Ratio γ	.764	.755	.720	.678	.604	.481	.32	
Groove Angle β, Degrees	18.6	18.5	18.4	18.3	18.2	17.8	18.	
Stability M	5.16	5.11	.977	.464	.210	.0884	.0329	
Radial Load Capacity F_r	.0366	.0366	.182	.359	.686	1.20	1.77	
Stability Ratio [1]	1.07	1.09	1.15	1.30	2.44	155.	571.	
Load Ratio [2]	.96	.96	.94	.92	.88	.80	.66	
Film Thickness Ratio H	2.54	2.53	2.47	2.44	2.42	2.48	2.12	1/2
Groove Width Ratio	.475	.471	.453	.436	.411	.392	.34	
Groove Length Ratio γ	.736	.721	.663	.600	.493	.339	.26	
Groove Angle β, Degrees	21.3	21.1	20.6	20.1	19.1	18.2	15.	
Stability M	9.32	9.14	1.70	.783	.336	.129	.0406	
Radial Load Capacity F_r	.0653	.0667	.354	.718	1.29	1.85	2.08	
Stability Ratio [1]	1.04	1.05	1.08	1.15	4.27	72.	100.	
Load Ratio [2]	.98	.97	.96	.95	.93	.80	.55	
Film Thickness Ratio H	2.37	2.36	2.31	2.30	2.32	2.52	3.77	1
Groove Width Ratio α	.493	.488	.471	.454	.425	.398	.158	
Groove Length Ratio γ	.685	.663	.591	.516	.410	.263	.268	
Groove Angle β, Degrees	26.0	25.7	24.5	23.2	20.7	19.4	9.7	
Stability M	14.3	13.9	2.50	1.12	.463	.170	.0510	
Radial Load Capacity F_r	.0992	.116	.735	1.33	1.91	2.47	2.81	
Stability Ratio [1]	1.02	1.10	3.13	1.06	2.86	6.91	3.83	
Load Ratio [2]	.98	.96	.84	.98	.93	.76	.50	
Film Thickness Ratio H	2.25	2.24	2.19	2.18	2.22	2.23	2.29	2
Groove Width Ratio α	.528	.528	.527	.526	.528	.500	.461	
Groove Length Ratio γ	.636	.607	.527	.467	.398	.346	.332	
Groove Angle β, Degrees	32.6	32.1	30.4	28.9	25.9	24.8	23.4	
Stability M	16.1	15.4	2.68	1.19	.509	.212	.0881	
Radial Load Capacity F_r	.112	.203	1.21	1.86	2.67	3.93	6.43	
Stability Ratio [1]	1.02	∞	1.32	1.05	1.22	1.43	1.65	
Load Ratio [2]	.99	.57	.91	.98	.90	.79	.71	

[1] $(M)_{\text{Max. Stability Brg}}/(M)_{\text{Max. Load Brg}}$

[2] $(F_r)_{\text{Max. Stability Brg}}/(F_r)_{\text{Max. Load Brg}}$

8

TABLE II: HERRINGBONE GROOVE PARAMETERS TO MAXIMIZE STABILITY - GROOVED MEMBER ROTATING

	INCOM-PRESSIBLE SOLUTION	COMPRESSIBLE SOLUTION BEARING COMPRESSIBILITY NUMBER Λ							LENGTH TO DIAMETER RATIO L/D
		1	2	5	10	20	40	80	
Film Thickness Ratio H [1]	4.	4.	4.	4.	4.	2.40	1.99	1.94	1/4
Groove Width Ratio α [2]	.6	.6	.6	.6	.6	.6	.6	.6	
Groove Length Ratio γ	1.	1.	1.	1.	1.	1.	1.	1.	
Groove Angle β, Degrees	11.4	11.7	11.9	12.2	12.2	32.4	59.0	74.4	
Stability M	8.64	9.79	5.71	4.41	4.41	1.37	.450	.125	
Radial Load Capacity F_r	.0314	.0313	.0626	.155	.305	.647	.750	.733	
Stability Ratio [3]	1.38	1.52	1.73	3.43	5.12	2.03	417.	1640.	
Load Ratio [4]	.83	.82	.82	.80	.79	.85	.54	.31	
Film Thickness Ratio H [1]	2.59	2.99	4.	4.	4.	4.	4.	4.	1/2
Groove Width Ratio α [2]	.6	.6	.6	.6	.567	.361	.295	.317	
Groove Length Ratio γ	1.	1.	1.	1.	1.	1.	1.	1.	
Groove Angle β, Degrees	23.4	19.6	13.7	14.0	11.8	11.8	10.0	8.69	
Stability M	11.9	13.1	8.02	7.28	5.74	2.30	1.14	.951	
Radial Load Capacity F_r	.0629	.0592	.0865	.210	.368	.638	.960	1.32	
Stability Ratio [3]	1.14	1.24	1.50	6.26	5.58	3.66	467.	3880.	
Load Ratio [4]	.94	.86	.61	.57	.50	.49	.48	.45	
Film Thickness Ratio H	2.17	2.25	2.37	2.54	2.54	3.10	3.06	2.77	1
Groove Width Ratio α [2]	.6	.6	.6	.6	.6	.6	.6	.478	
Groove Length Ratio γ	1.	1.	1.	1.	1.	1.	1.	.904	
Groove Angle β, Degrees	36.0	36.2	35.6	34.1	34.1	22.0	21.8	24.2	
Stability M	16.6	18.4	10.6	8.61	8.61	6.44	6.39	3.94	
Radial Load Capacity F_r	.0899	.0973	.194	.424	.654	.694	.997	2.87	
Stability Ratio [3]	1.10	1.39	∞	13.6	8.52	9.47	299.	779.	
Load Ratio [4]	.89	.79	.61	.49	.49	.37	.37	.68	
Film Thickness Ratio H	2.06	2.12	2.22	2.46	2.50	2.54	2.68	2.68	2
Groove Width Ratio α [2]	.6	.6	.6	.6	.6	.6	.6	.6	
Groove Length Ratio γ	.831	.900	.976	1.	1.	1.	1.	.949	
Groove Angle β, Degrees	43.1	46.6	50.3	54.4	55.0	57.6	63.7	66.1	
Stability M	17.7	18.6	10.0	6.19	6.14	5.99	4.71	3.72	
Radial Load Capacity F_r	.107	.150	.278	.461	.626	.830	1.00	1.69	
Stability Ratio [3]	1.04	∞	∞	3.31	5.29	10.1	19.4	42.7	
Load Ratio [4]	.94	.42	.37	.35	.35	.32	.24	.23	

[1,2] Maximum H of 4 and α of .6 considered in analysis

[3] $(M)_{\text{Max. Stability Brg}}/(M)_{\text{Max. Load Brg}}$

[4] $(F_r)_{\text{Max. Stability Brg}}/(F_r)_{\text{Max. Load Brg}}$

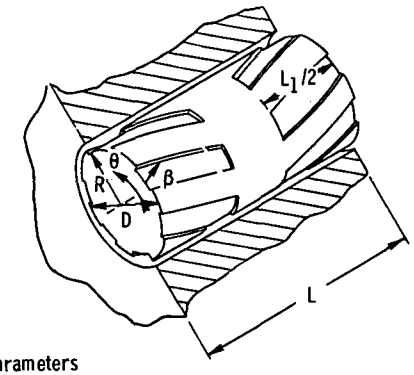

Bearing parameters

1. $\lambda = \frac{L}{D}$

2. $\Lambda = \frac{6\mu\omega R^2}{p_a h_r^2}$

Groove parameters

1. $H = \frac{h_g}{h_r}$

2. $\alpha = \frac{b_g}{b_g + b_r}$

3. β

4. $\gamma = \frac{L_1}{L}$

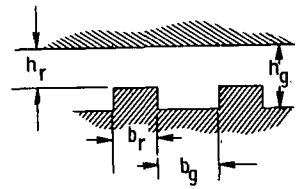

Figure 1. - Schematic of a concentric herringbone journal bearing.

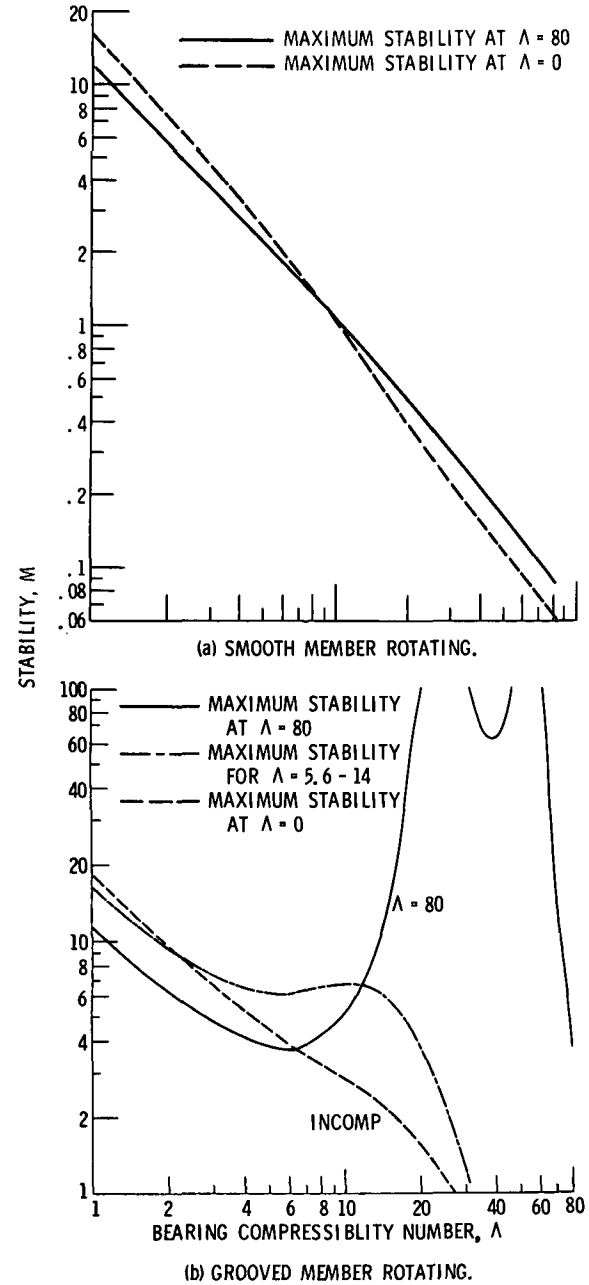

Figure 2. - Typical stability curves for optimized bearings, L/D = 2.

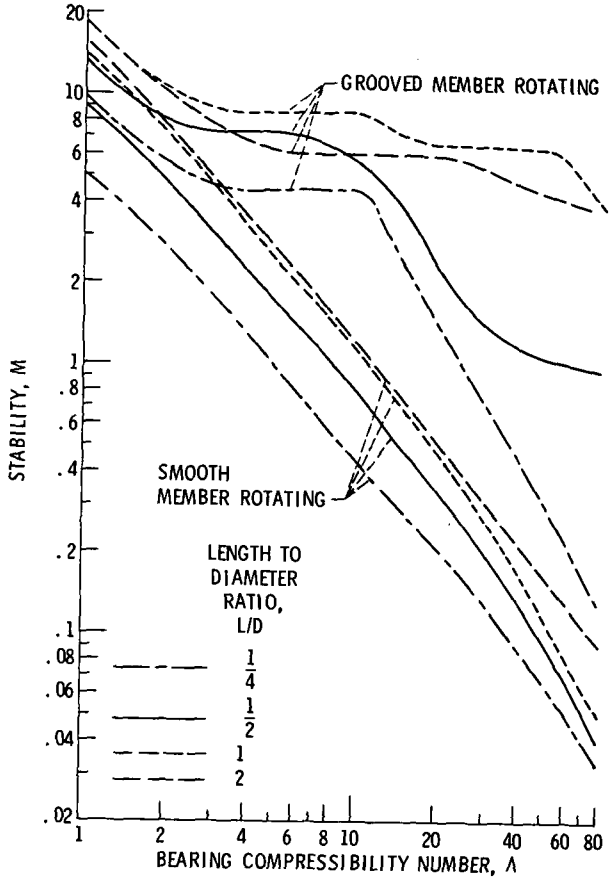

Figure 3. - Maximum stability of herringbone grooved bearings.

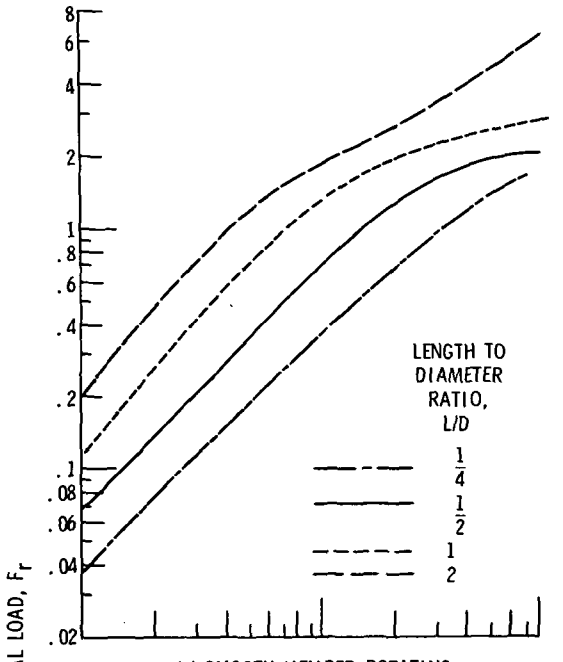

(a) SMOOTH MEMBER ROTATING.

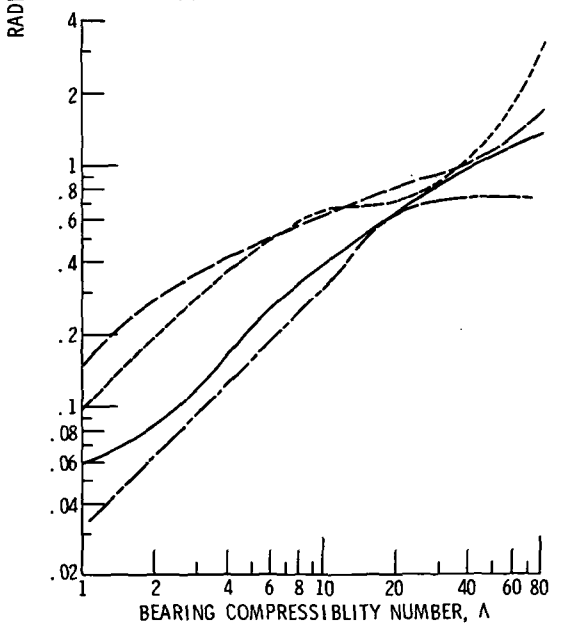

(b) GROOVED MEMBER ROTATING.

Figure 4. - Radial load capacity of maximum stability bearings.

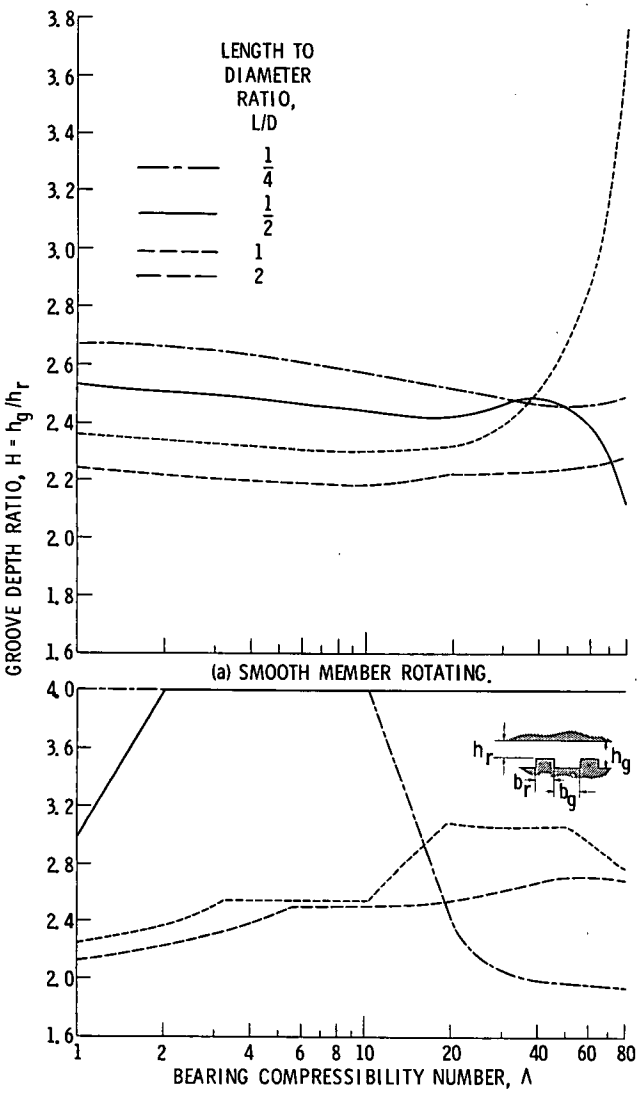

Figure 5. - Groove depth ratios to maximize stability.

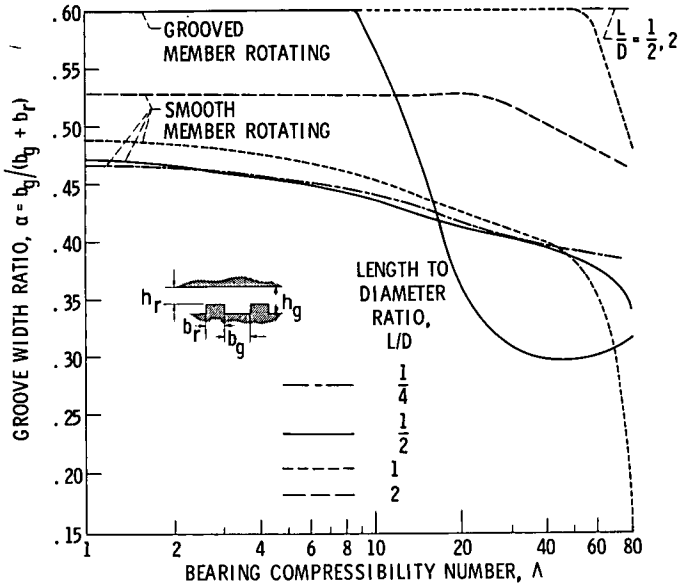

Figure 6. - Groove width ratios to maximize stability.

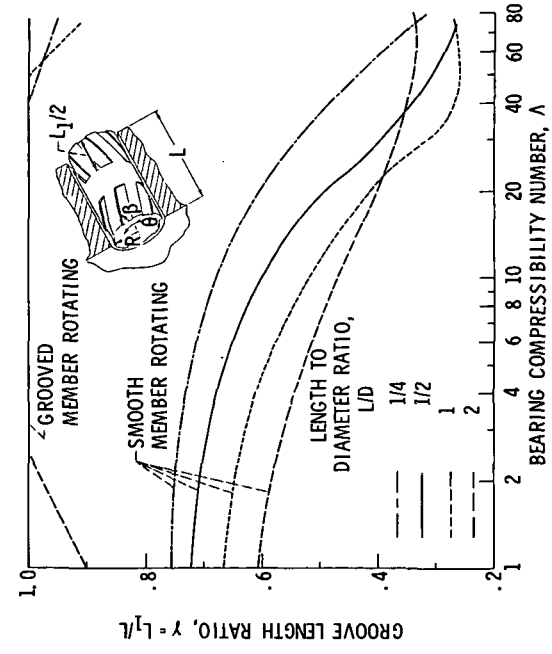

Figure 7. - Groove length ratios to maximize stability.

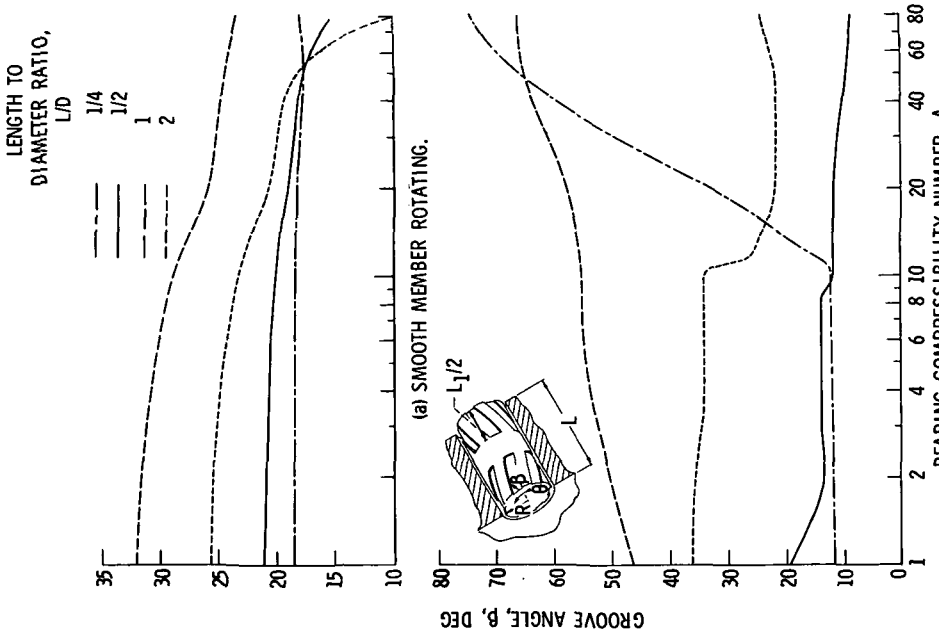

Figure 8. - Groove angles to maximize stability.